Rafting microstructure during creep of the MC2 nickel-based superalloy at very high temperature

Fabienne Touratier[a,b], Eric Andrieu[a], Dominique Poquillon[a], Bernard Viguier[a,*]

[a] CIRIMAT-CNRS/UPS/INPT, 118 route de Narbonne 31077 Toulouse Cedex 04 France
[b] TURBOMECA, avenue du 1er mai, 40220 Tarnos, France

A B S T R A C T

Directional coarsening of the single-crystalline nickel-based superalloy MC2 has been investigated by means of tensile creep tests at 1100 °C. Two specific specimen geometries were designed in order to generate a variety of stress and strain states. Different coarsening microstructures are observed: N- and P-type classical rafting but also coarsening oriented 45° away from the load axis. The comparison of microstructure maps with the local mechanical state evaluated by finite element calculations shows that the 45° directional coarsening appears in case of very high cumulated strain values (above 10%), independent of the stress sign. Transmission electron microscopy investigations show that the dislocation microstructure is similar in both N-type and 45° coarsened areas.

Keywords:
Single crystal nickel-based superalloy
High temperature creep test
Rafting
Stress and strain states

1. Introduction

Single-crystalline nickel-based superalloys are currently used in turbine blades of aircraft and helicopter. They were designed to resist to the severe operation conditions of those parts exposed to load at high temperature of about 1000 °C. In emergency situations, especially for helicopters, the temperature can even increase drastically up to 1200 °C. The optimized microstructure of superalloys consists of a high volume fraction [1] of cuboidal γ' precipitates ($L1_2$ ordered cubic phase, lattice parameter $a_{\gamma'}$) coherently embedded in the γ matrix (fcc disordered phase, lattice parameter a_γ). However, after short time exposure to service conditions, an anisotropic evolution of this microstructure, known as directional coarsening or rafting, occurs [2,3]. These rafts lie in cubic {0 0 1} planes and their orientation depends on the sign of the stress and of the misfit δ of the material defined as: $\delta = 2[a_{\gamma'} - a_\gamma]/[a_{\gamma'} + a_\gamma]$. When a [0 0 1] tensile stress is applied on a negative misfit material, the effective stress in the horizontal channels is greater than in the vertical channels [4,5]. This promotes creep dislocation motion in the horizontal channels and relaxes the internal stresses [6–8] in these channels thus stabilizing the microstructure. The result is the coalescence of the vertical matrix channels, i.e., rafting [9] perpendicularly to the tensile [0 0 1] stress, called N-type rafting. When a compressive stress is applied, rafting occurs in parallel direction to the [0 0 1] stress, and this is called P-type rafting.

* Corresponding author. Tel.: +33 562 885 664; fax: +33 562 885 663.
E-mail address: Bernard.Viguier@ensiacet.fr (B. Viguier).

However, precipitate interfaces reoriented 45° away from the tensile axis have sometimes been reported, particularly near the rupture zone after high temperature creep tests [10,11]. A microstructure totally reoriented at 45° from the applied stress was also observed in the macroscopic crystallographic shear system $\{0\,1\,1\}\langle 0\,1\,\bar{1}\rangle$ [12,13]. In this case, rafts are fully reoriented on the whole shear zone. The authors denoted that the shear stress can be decomposed in its maximum principal stresses and so, γ' particles coarsen as usual for a negative misfit: perpendicular to the tensile principal stress and parallel to the compressive one. Finally, Dryepondt [14] observed such 45° coarsening during creep to rupture in tensile conditions at 1150 °C–80 MPa. The microstructure reveals bands of several rows of precipitates reoriented at 45° from the [0 0 1] axis which seem to provoked the failure of the sample. Between these bands, some precipitates show interfaces reoriented at 45°, within a microstructure mainly composed of N-type coarsened precipitates as expected. The mechanism leading to such "unusual" coarsening was not elucidated. The aim of the present work is to study this 45° coarsening by means of high temperature interrupted tensile creep tests. Specific sample geometries were designed and modelled using finite element calculations to determine the macroscopic conditions leading to this phenomenon. Transmission electron microscopy (TEM) examinations were performed for studying the microscopic mechanisms involved.

2. Experimental part

The material studied was taken from a MC2 single crystal plate (120 mm × 60 mm × 12 mm)[15] (nominal composition

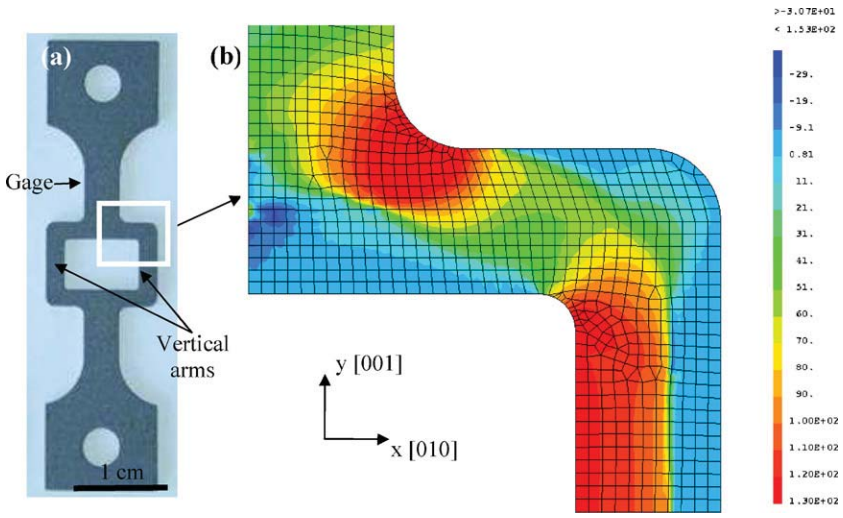

Fig. 1. (a) Sketch of the hollow sample. (b) Finite elements simulation of the largest principal stress σ_{11} for a quarter of the sample. (Scale is given in MPa).

Ni–7.2Cr–8Co–2Mo–7W–5.5Al–1.3Ti–5.6Ta in wt.%) provided by Turbomeca and showing a slight disorientation (7°) between its longitudinal axis and the [0 0 1] axis. Adequate heat treatments (3 h 1300 °C–6 h 1080 °C–20 h 870 °C) were performed on this plate so that the microstructure consists of an homogeneous distribution of cuboidal γ′ particles aligned along the ⟨0 0 1⟩ directions with a mean edge length of 440 nm. Thin planar specimens with two different shapes (1 and 1.2 mm in thickness) were electro-discharge machined (Fig. 1a and 4a) and mechanically grinded with SiC paper. The plane of the specimen roughly corresponds to (1 0 0) and load is applied along the longitudinal axis of the plate (close to [0 0 1]). High temperature tensile creep tests were carried out under laboratory air at 1100 °C in a radiation furnace which allows high heating and cooling rates on a creep frame loaded with a constant load [16].

For the hollow sample (Fig. 1a), creep tests were performed at 1100 °C and 62 N for 24 h and for the notched sample (Fig. 4a) at 1100 °C and 580 N for various durations corresponding to increasing cumulated strain (see Section 3.2). Finite element simulation was performed on these samples using the FE code CAST3 M [17]. Isothermal (1100 °C) two dimensional plane stress calculations were carried out, based on isotropic elasticity for the linear behavior and on a Norton creep law for the non linear behavior. Plastic data were taken at 1100 °C for the MC2 alloy: Young's modulus $E_{MC2\ 1100°C} = 71{,}300$ MPa and Poisson's ratio $\nu = 0.33$. Tensile creep tests on flat specimens with constant cross section were realized to determine the creep law. For $T = 1100$ °C and stress values of 80, 140 and 154 MPa, creep was shown to obey a Norton law $\dot{\varepsilon} = A\sigma^n$ with $A = 2.06 \times 10^{-29}$ and $n = 10.34$. Loading during simulations is achieved within one second according to the experimental procedure. So, during loading, only elastic behavior is considered. After creep tests, samples were mechanically grinded with SiC paper to remove the oxide layer formed at high temperature, then polished with diamond paste down to 1 μm and etched with a positive attack (13% H_3PO_4, 45% H_2SO_4 and 42% HNO_3 under 3 V) so that the γ matrix is preferentially attacked. Microstructure observations were achieved using the stage for macrography of an Olympus optical microscope and a LEO 435 VP scanning electron microscope operating at 15 kV.

TEM samples with $(2\,\bar{1}\,\bar{1})$ plane normal were extracted from the notched samples using a diamond saw. These slices of original thickness $e = 200$ μm were mechanically grinded down to about 50 μm thickness, then dimpled to about 20 μm and finally ion milled using a PIPS (Gatan). The observations were realized on a Jeol 2010

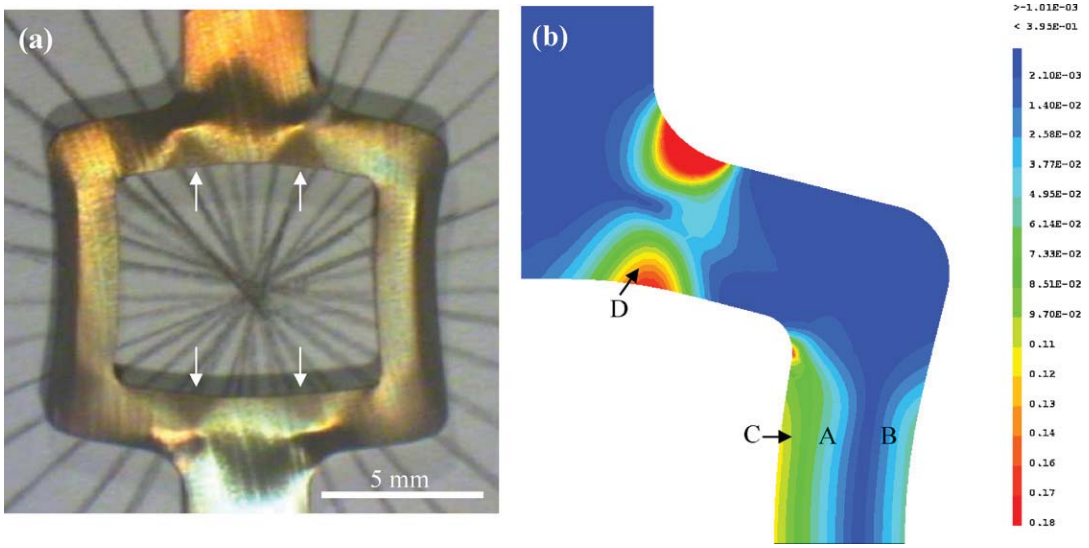

Fig. 2. (a) Optical image of the hollow sample after creep test (1100 °C, 62 N, 24 h) and etching. (b) Map of the equivalent plastic strain obtained by finite elements simulation.

Table 1
Stress and strain values at the different locations labeled in Fig. 2 at the end of the creep (1100 °C, 62 N, 24 h) in the hollow sample.

Location in the sample	σ_{VM} after creep (MPa)	σ_{11} (MPa)	σ_{22} (MPa)	σ_{XY} (MPa)	$\sigma_{\text{hydrostatic}}$ (MPa)	ε_{eq}	ε_{YY}	ε_{XX}
A	115	115	0.2	−0.05	38	4%	3%	−3%
B	115	0	−110	0.04	−36	3%	−3%	2%
C	130	128	−0.02	−0.02	42	10%	11%	−5%
D	130	2	−132	5	−40	15%	7%	−14%

operating at 200 kV at the TEMSCAN service of the Université Paul Sabatier in Toulouse.

3. Results

3.1. The hollow sample

The hollow sample (Fig. 1a) was designed to generate a large variety of stress and strain states in the same sample. Finite element maps of the Von Mises stress, the principal stresses σ_{11} and σ_{22} with their directions, the shear stress, the stress triaxiality, the strain along the X and Y axes and the equivalent plastic strain ($\varepsilon_{\text{eq}} = \sqrt{(2/3)(\underline{\underline{\varepsilon}}^{\text{p}}\underline{\underline{\varepsilon}}^{\text{p}})}$ where $\underline{\underline{\varepsilon}}^{\text{p}}$ is the cumulated plastic strain tensor [18]) were calculated for an applied load of 62 N at 1100 °C for 24 h. Fig. 1b illustrates such calculations with the maximum principal stress σ_{11}. On the sample, different states of stress are generated such as tensile states ranging roughly from 20 MPa on the gage to 130 MPa in the vertical arms (Fig. 1), compressive states on the majority on the horizontal arms and on the external part of the vertical ones (around 120 MPa) and even pure shearing bands with a stress of 60 MPa oriented at 45° from the applied stress.

Fig. 2a is a macrograph obtained with grazing light which shows the crept hollow sample after etching (1100 °C, 62 N, 24 h). We can notice that the contrast highlights several areas which appear bright or dark on the picture. Four black triangles appear on the horizontal parts of the sample, as shown by white arrows in Fig. 2a. On the vertical arms, etching underlines two areas: a bright one on about two third of the arm in the inner side and a dark one in the outer side. It will be shown below that this contrast arises from the different coarsening of the microstructure. This microstructure overview is compared to the map of the cumulated equivalent plastic strain plotted in Fig. 2b where the cumulated plastic strain ranges from 0 to 15% after the simulation of the 24 h creep test. This strain map allows highlighting different areas which fit very well with the ones visualized by etching in Fig. 2a. Thus, we can notice that the four triangle shapes are the most strained zones in the whole sample (about 15%), the very internal sides of the vertical arms (at about 450 μm from the hole) are 10% strained whereas the rest of the sample is 0 to 5% strained.

The coarsening microstructure is more accurately observed using scanning election microscopy (SEM) on different areas defined here below. The middle of the vertical arm (labeled A in Fig. 2b) under tensile stress, and the external part (labeled B in Fig. 2b) under compressive stress, are respectively N or P-coarsened (Fig. 3a and b) as expected. However, in the C zone (Fig. 2a) in which tensile stress is found, SEM images reveal at about 450 μm a high tendency to 45° directional coarsening (Fig. 3c). This tendency to 45° coarsening is less pronounced when moving away from the hole to reach continuously the classical N coarsening of zone A. Finally, the four black triangular shapes (D zone) correspond to directional coarsening oriented 45° away from the load axis (Fig. 3d). This feature is generalized in all dark triangular areas and presents some

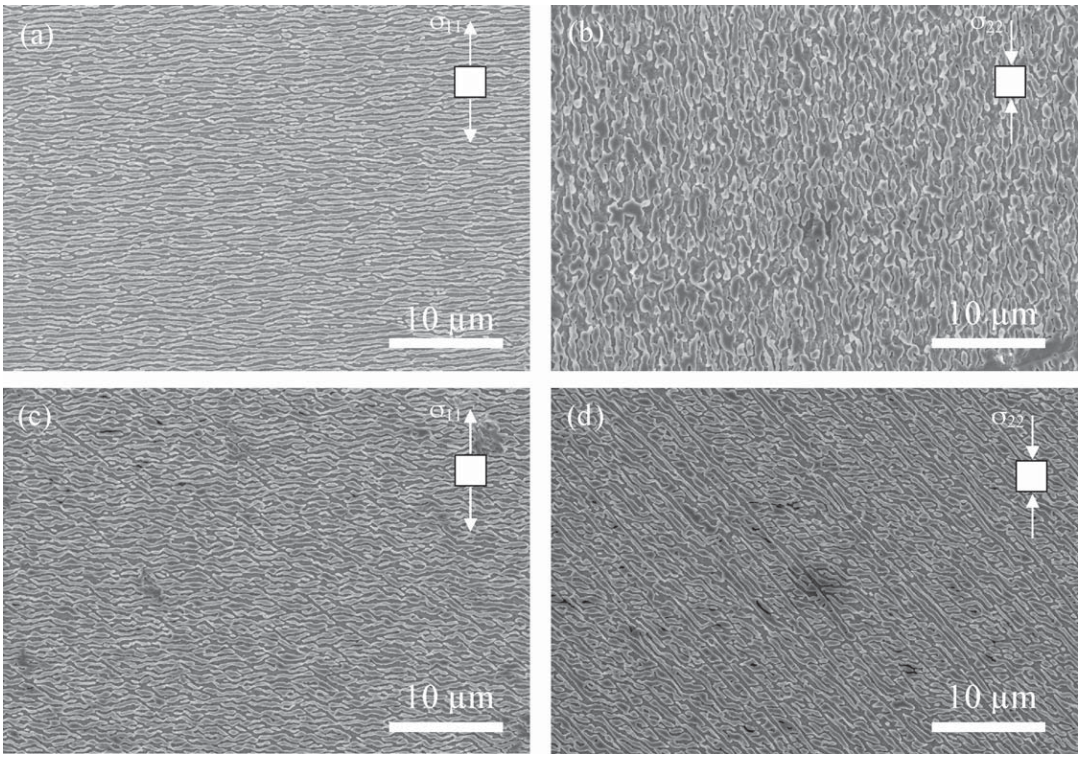

Fig. 3. SEM images of the hollow sample microstructure (a) in the middle of the vertical arm (A), (b) on the external side of the vertical arm (B), (c) on the internal side of the vertical arm (C), and (d) in a black triangle (D). The sketch in the upper right corner of each micrograph represents the plane stress state in this area.

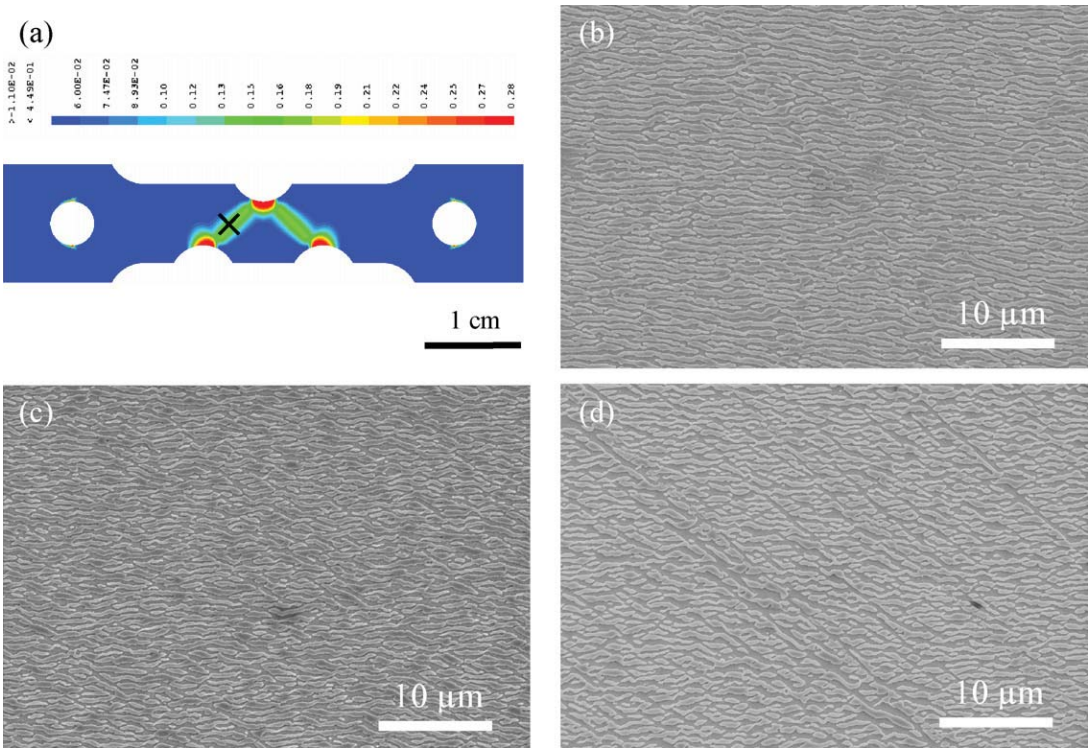

Fig. 4. (a) Finite elements simulation of the equivalent plastic strain for the notched sample and SEM images of the area between 2 notches (black cross) after creep test at 1100 °C and 580 N, (b) interrupted at the beginning of the secondary stage, (c) interrupted at the end of the secondary stage and (d) after the failure.

long γ′ precipitates totally reoriented whereas the others just show some interfaces at 45°. Values of stress and strain extracted from the simulation on different locations are listed in Table 1. It is noticeable that 45° directional coarsening appears whatever the sign of the stress is because we find it in tensile (C) and compressive (D) areas (Fig. 1b), and that it concerns the most strained areas in the sample (Fig. 2b). These results are reasonable because for this specific geometry the strain is concentrated particularly in the areas with triangle shape which are stressed in compression and therefore delay crack formation and so the rupture of the sample. So, very high strain values for MC2 can be reached and localized in specific areas of the specimen (15%), contrary to tensile loading on constant cross section specimens where rupture occurs at about 10%.

3.2. *The notched sample*

This second geometry was designed to produce 45° directional coarsening on wider areas than the ones of the hollow sample. FE calculations presented in Fig. 4a clearly show that during creep, strain is not homogeneous but concentrates between notches on

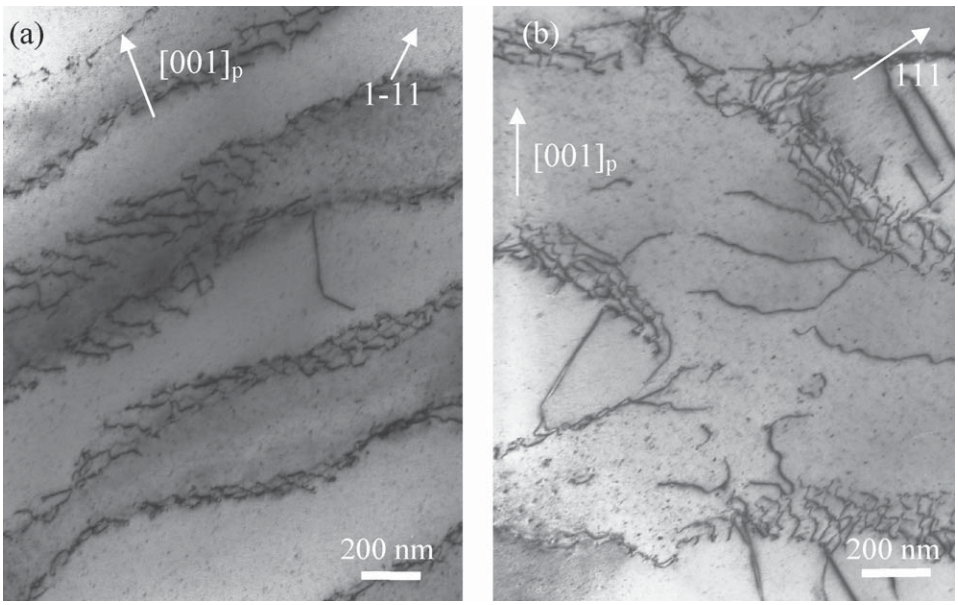

Fig. 5. TEM images showing the morphology of dislocations after creep tests at 1100 °C and 580 N (a) interrupted at the end of the primary stage after 19 h (b) after the failure (70 h). The direction $[0\,0\,1]_p$ indicates the projected direction of the [0 0 1] axis on the picture plane.

highly strained bands (at 45° from the longitudinal axis of the specimen). In this geometry, creep tests realized at 1100 °C and 580 N (which corresponds to a stress of 60 MPa on the maximal width of the gage) result in classically shaped creep curve with primary, secondary and tertiary stages. Further creep tests were realized and interrupted at different stages of the creep curve. The first one was interrupted after 19 h in the beginning of the secondary stage. The microstructure obtained is shown Fig. 4b and presents a classical N coarsening consistent with the tensile stress. The second one interrupted after 45 h at the transition from secondary to tertiary creep (Fig. 4c) shows an evolution: obviously, the rafts are N coarsened but some precipitates with interfaces reoriented 45° away from the load axis begin to appear. Finally, the last creep test conducted until rupture after 70 h shows (Fig. 4d) a clear 45° directionally coarsened microstructure with the apparition of bands of several precipitates totally reoriented whereas the rest of the rafts is quite similar to Fig. 4c. All the images were taken at the same location, in the band concentrating the strain between the notches (see black cross Fig. 4a).

TEM studies were performed between the two notches on the sample interrupted in the primary stage after 19 h and on the one crept to rupture (Fig. 5). In both cases, ½ ⟨1 1 0⟩ dislocations are observed. The first sample which only shows a N-type microstructure presents arrays of dislocations surrounding the γ′ precipitates. Burgers vectors of ½ [0 1 1] and ½ [1 0 1] were identified despite the precise structure of the interfacial network was not elucidated. For the sample crept until rupture, the zones located in the matrix between two γ′ interfaces oriented 45° away from the load axis mainly show ½ [1 1 0] and ½ [1 0 1] Burgers vectors.

4. Discussion

Following the results in the literature [10–14] we have shown that rafting of γ′ precipitates in superalloys which is usually observed to occur on {0 0 1} planes can be observed 45° away the [0 0 1] normal stress, that is rafts lie on {1 1 0} planes. Such "unusual" coarsening has been observed repeatedly in highly strained zones, that is 45° coarsening is associated with a high strain accumulation and is independent of the stress sign as it appears in both compressive and tensile stressed areas (contrary to usual rafting which strongly depends on the sign of the stress). According to the notched specimen behavior, it appears that 45° directional coarsening results from an evolution of the microstructure: for relatively low strain values ($\varepsilon < 10\%$) a classical rafting microstructure sets up depending on the sign of the stress (leading to N or P rafting as usually observed); when high strain values are reached ($\varepsilon > 10\%$ as it is the case in our specific samples or close to the rupture zone of usual specimen), a destabilization of the microstructure occurs which progressively leads to the 45° coarsening microstructure. At this stage, it is not clear whether this reorientation of the rafts occurs by a dissolution/reprecipitation mechanism or some kind of rocking mechanism by shearing of the precipitates. However the reorientation always starts by the rotation of interfaces at the ends of rafts, which then proceeds with the rotation of the whole precipitates. This phenomenon is first observed on localized rows then bands which further generalize over the whole highly strained area.

The comparison of local mechanical state (σ, ε) obtained by FE calculation and the microstructure map deduced from observations shows that the occurrence of 45° coarsening needs large plastic strain values. The explanations given by Kamaraj et al. [12,13] seem not to apply in the present case, since we observed such anomalous coarsening in areas where FE calculations show that the principal stresses are always parallel to ⟨1 0 0⟩ directions (e.g., zone C in Figs. 2b and 3c). We believe that Kamaraj et al. [12,13] could observe 45° coarsening because they used shearing specimens where strain is concentrated and thus are reached higher strain values than for tensile testing. Besides, a striking observation is that the simple isotropic model used for FE calculations leads to a mapping of plastic strain which accurately fit the different microstructure domains observed. This observation suggests that plastic strain values obtained under creep conditions at high temperatures obey an isotropic behavior. Accordingly, it has been shown [19–21] that the strong anisotropic creep behavior of single crystals observed during primary creep at low temperature becomes less important for higher temperatures and strain levels. Another relevant observation concerns the role of time versus the plastic deformation. Indeed, specimen showing black triangle shapes experienced creep test for 24 h and presents 45° coarsening strongly whereas in the notched sample, after 45 h creeping, the microstructure is still mainly N-type rafted with only some γ/γ′ interfaces reoriented at 45°. The 45° destabilization is only visible at rupture after 70 h testing. This emphasizes the predominant role of the plastic strain compared to time as regard to the destabilization of the classical rafted microstructure to form 45° coarsening. As recognized by Pineau [22], the sign of the applied stress (tensile or compressive) dictates the microstructure of classical rafting (N or P) as we observed in the moderately strained areas whereas, for larger plastic strains, the 45° destabilization occurs, whatever is the sign of the stress. Furthermore, the preliminary TEM observations indicate that this behavior is associated with the operation of classical ½ ⟨1 1 0⟩ dislocations whatever is the shape of the coarsen precipitates. Work is in progress on the microstructural features that may explain this behavior.

5. Conclusion

A rafted microstructure where γ′ precipitates are oriented 45° away from the load axis is highlighted in this study. This phenomenon is easily reproducible in high-temperature tensile creep tests thanks to specific samples which were designed to localize plastic strain. FE calculations allowed us to identify and localize different stress states and match them with corresponding microstructure evolution. Contrary to N-type or P-type coarsening, 45° rafting is independent of the sign of the stress and appears if strain values are higher than 10%. As the accumulation of strain increases, an evolution of the N or P microstructure occurs and progressively leads to the 45° coarsened microstructure. TEM studies show that the dislocation structures seem to be identical between a sample showing N-type coarsening and a sample showing 45° coarsening.

Acknowledgements

The authors acknowledge the company TURBOMECA–groupe SAFRAN and J-C Garcia for financial support and for providing the material. The authors also acknowledge the referee's detailed reading and relevant comments on the manuscript.

References

[1] T. Murakumo, T. Kobayashi, Y. Koizumi, H. Harada, Acta Mater. 52 (2004) 3737–3744.
[2] J.K. Tien, S.M. Copley, Metall. Trans. 2 (1971) 215–219.
[3] D.D. Pearson, F.D. Lemkey, B.H. Kear, in: M. Park (Ed.), Proceedings of the 4th International Symposium on Superalloys, ASM, OH, 1980, pp. 513–520.
[4] A. Royer, A. Jacques, P. Bastie, M. Veron, Mater. Sci. Eng. A 319–321 (2001) 800–804.
[5] L. Muller, U. Glatzel, M. Feller-Kniepmeier, Acta Metall. Mater. 40 (1992) 1321–1327.
[6] C. Carry, PhD thesis, Ecole Nationale Supérieure des Mines de Paris, Paris, 1976.
[7] J.Y. Buffière, PhD thesis, Institut National Polytechnique de Grenoble, Grenoble, 1993.
[8] M. Veron, PhD thesis, INP Grenoble, Grenoble, 1995, p. 172.
[9] T.M. Pollock, A.S. Argon, Acta Metall. Mater. 42 (1994) 1859–1874.

[10] M. Feller-Kniepmeier, T. Link, Metall. Trans. A 20 (1989) 1233–1238.
[11] A. Epishin, T. Link, P.D. Portella, U. Bruckner, Acta Mater. 48 (2000) 4169–4177.
[12] M. Kamaraj, C. Mayr, M. Kolbe, G. Eggeler, Scripta Mater. 38 (1998) 589–594.
[13] M. Kamaraj, Sadhana 28 (2003) 115–128.
[14] S. Dryepondt, PhD thesis, INP Toulouse, Toulouse, 2004.
[15] P. Caron, T. Khan, in: E. Exner, V. Schumacher (Eds.), Proceedings of the First European Conference on Advanced Materials and Processes, EUROMAT, Aachen, Germany, 1989, pp. 333–338.
[16] S. Dryepondt, D. Monceau, F. Crabos, E. Andrieu, Acta Mater. 53 (2005) 4199–4209.
[17] http://www-cast3m.cea.fr/cast3m/index.jsp.
[18] D. François, A. Pineau, A. Zaoui, Comportement mécanique des matériaux, Ed. Hermés, Paris, 1995, p. 332.
[19] P. Caron, Y. Ohta, Y.G. Nakagawa, T. Khan, in: D.S. Reichman, G. Maurer, S. Antolovich, C. Lund (Eds.), Superalloys 1988, The Metall. Society of AIME, Warrendale, PA, 1988.
[20] V. Sass, U. Glatzel, M. Feller-Kniepmeier, Acta Mater. 44 (1996) 1967–1977.
[21] V. Sass, U. Glatzel, M. Feller-Kniepmeier, in: Superalloys 1996, R.D. Kissinger, D.L. Anton, A.D. Cetel, M.V. Nathal, T.M. Pollock and D.A. Woodford (Eds.), The Minerals, Metals and Materials Society, 1996, pp. 283–290.
[22] A. Pineau, Acta Metall. 24 (1976) 559–564.